Aerosol and Air Quality Research

ORIGINAL RESEARCH
https://doi.org/10.4209/aaqr.230180

Influence of Test Protocol on Filtration Efficiency of Medical Face Mask Material

Aurélie Joubert *, Ala Bouhanguel, Yves Andrès, Laurence Le Coq

IMT Atlantique, GEPEA, CNRS UMR 6144, 4 Rue Alfred Kastler, CS 20722, F-44307 Nantes, France

ABSTRACT

Medical face masks are an efficient protective barrier against the propagation of bacteria and viruses in societies. The current European standard focuses on the bacterial filtration efficiency of the filtering material for a mean particle size of 3.0 μm in terms of droplets that are exhaled, but viruses that are inhaled can be transported by particles of sub-micron size. The filtration efficiency of medical face mask material was evaluated in a bench test from both unused charged and discharged masks. Several polydisperse test aerosols were used - DEHS, alumina, HOLI, NaCl, *Staphylococcus epidermidis* and *Emesvirus zinderi* (MS2) - produced by liquid atomization and/or powder dispersion, and sized by optical and aerodynamic counters or cascade impactors. The results have shown that the particle size distribution and charges for a given type of aerosol can differ depending on the generator used, in particular the wet or dry nature of generation. The results in the sub-micron size range for charged face mask material showed that the filtration efficiency of neutral aerosols was lower than that of charged aerosols due to the electrostatic forces, e.g., 92% versus 99% efficiency for DEHS and alumina respectively for a mean aerodynamic diameter of 0.6 μm. With the discharged face mask material, the filtration efficiency was degraded in the sub-micron size range for all types of aerosol tested: e.g., 30% versus 65% efficiency for a mean optical diameter of 0.25 μm respectively for DEHS and alumina. For particle sizes > 3 μm, the results indicated that the nature of the aerosol has little influence because particle collection is dominated by impaction and interception mechanisms. The tests with MS2 virus demonstrated a good fit with NaCl filtration efficiency expressed in aerodynamic diameters over a range between 0.65 and > 7 μm, for charged and discharged medical face mask materials.

Keywords: Test aerosols, MS2 virus, Electrostatic charges, Particle collection mechanisms

Received: July 28, 2023
Revised: October 27, 2023
Accepted: November 22, 2023

* **Corresponding Author:**
aurelie.joubert@imt-atlantique.fr

Publisher:
Taiwan Association for Aerosol Research
ISSN: 1680-8584 print
ISSN: 2071-1409 online

1 INTRODUCTION

Global changes, including climate change, globalization and anthropogenic pressure on the environment, are leading to the emergence and spread of infectious diseases such as the Covid-19 viral pandemic (Baker *et al.*, 2022). One major transmission mode occurs via human respiratory droplets ranging from 0.1 to 1000 μm, with an aerosol range of 0.1 to 10–20 μm. Smaller droplets can become vectors for viral contamination as they evaporate quickly and can be transported over long distances. Once aerosolized, the virus can also be adsorbed by airborne particles, which can modify the aerodynamic behavior and increase dispersion (Prather *et al.*, 2020).

The size of the respiratory droplet containing the virus may affect the response. Liu *et al.* (2020) investigated the aerodynamic nature of SARS-CoV-2 by measuring viral RNA in aerosols with a five-stage cascade impactor in different areas of two Wuhan hospitals. Peak concentrations of SARS-CoV-2 aerosols were found in rooms for removing protective apparel in the ranges 0.25 to 0.5 μm, 0.5 to 1.0 μm range and > 2.5 μm.

Medical face masks are widely used as a source-control device to reduce the transmission of viruses such as SARS-CoV-2 in the global Covid-19 pandemic. The source-control efficiency of medical face masks depends on the filtration efficiency of the filtering material and on the facial

adjustment of the mask. In Europe, medical face masks are certified by standard EN 14683:2019, which evaluates the performance of the filtering material without considering how the mask fits. The standard defines performance requirements for the filtering materials, in particular a bacterial filtration efficiency level for a mean particle size of 3.0 ± 0.3 μm (*Staphylococcus aureus*). US standard ASTM F2100-19 defines performance levels in particular for bacterial filtration efficiency and sub-micron particulate filtration efficiency at 0.1 μm from latex particles and optical counting. As with the US standard, Chinese standard YY/T 0469-2011 imposes requirements in terms of particle filtration efficiency at 0.1 μm.

Unlike medical face masks, protection devices such as FFPx (EN 149:2009) and N95 respirators, while effective in controlling aerosol emissions from the wearer, are primarily used to protect the wearer from exposure. Standards take into account the facial adjustment of the device with a leakage test. EN 149:2009 evaluates the filtration efficiency of the filtering material with sodium chloride (particle sizes range from 0.02 μm to 2 μm and have a mean aerodynamic diameter by mass of 0.6 μm) and paraffin oil (mean diameter of 0.4 μm).

Although little is known about facial leakage in relation to medical face masks, ill-fitting masks can lead to viral transmission by the wearer due to outward leaks, or viral contamination of the wearer due to inward leaks (Bahloul *et al.*, 2021; Kähler and Hain, 2020).

Medical face masks are composed of several non-woven layers of synthetic materials such as polypropylene fibers. Electrostatic charges (positive and negative) are added to the middle layer (e.g., by corona effect) to increase the particle collection efficiency. Particle collection by the face mask media is accomplished by several capture mechanisms: Brownian diffusion for small particles agitated by Brownian motion, direct interception for bigger particles driven close to the fibers, and impaction for the biggest particles with high inertia and leaving airflow lines through the media (Brown, 1993; Dahneke, 1971; Davies, 1973). The most penetrating particle size (MPPS) zone covers particles approximately 0.1–0.5 μm in diameter for mechanical media. With charged fibers and/or particles, the MPPS zone is shifted towards smaller particle diameters due to the enhancement of filtration efficiency by electrostatic forces: coulombic forces with charged fibers and particles, polarization forces with charged fibers and neutral particles, image forces with neutral fibers and charged particles (Romay *et al.*, 1998; Spielman, 1977; Wang, 2001).

In conclusion, medical face masks are used to limit contamination from the wearer to the environment, but are sometimes used as respiratory protection masks. Moreover, there is no consensus on the size of pathogenic organisms, such as viruses, that a protective mask should protect against. The test protocols for medical face mask standard focus on a particle size of 3 μm, whereas a characterization of the spectral filtration efficiency of medical masks as a function of particle size would be necessary. Finally, test protocols need to take into account of the many parameters that can influence the filtration efficiency of a medical face mask which are electret, in particular those affecting electrostatic forces during the filtration process.

The aim of this study is to evaluate the influence of the test protocol on the filtration efficiency of medical face mask filtering material for a wide range of particle sizes, including particle diameters of 3.0 μm. Several parameters were investigated: the nature of the test aerosol in terms of its physical properties, such as electrostatic charge; the method of aerosol generation; the method of counting and equivalent diameter considered and the filtering material charge. The tests were carried out with unused charged and discharged medical face mask material. To extrapolate to a live aerosol scenario, this study also included the investigation of microbial filtration regarding the bacteriophage MS2 virus as surrogate for SARS-CoV-2.

2 METHODS

2.1 Experimental Setup

The bench used to measure mask filtration efficiency (Whyte *et al.*, 2022a) included a centrifugal fan to suck air through a modular test section (Fig. 1). The air was first sucked in through a circular duct 7 cm in diameter and across a 100 cm length. For better mixing and homogenization of the flow, aerosols were injected into this narrow section with a turbulent flow regime ($Re > 80000$). The mixture (air/aerosol) was driven via a slightly diverging nozzle (angle $< 7\%$) towards a square

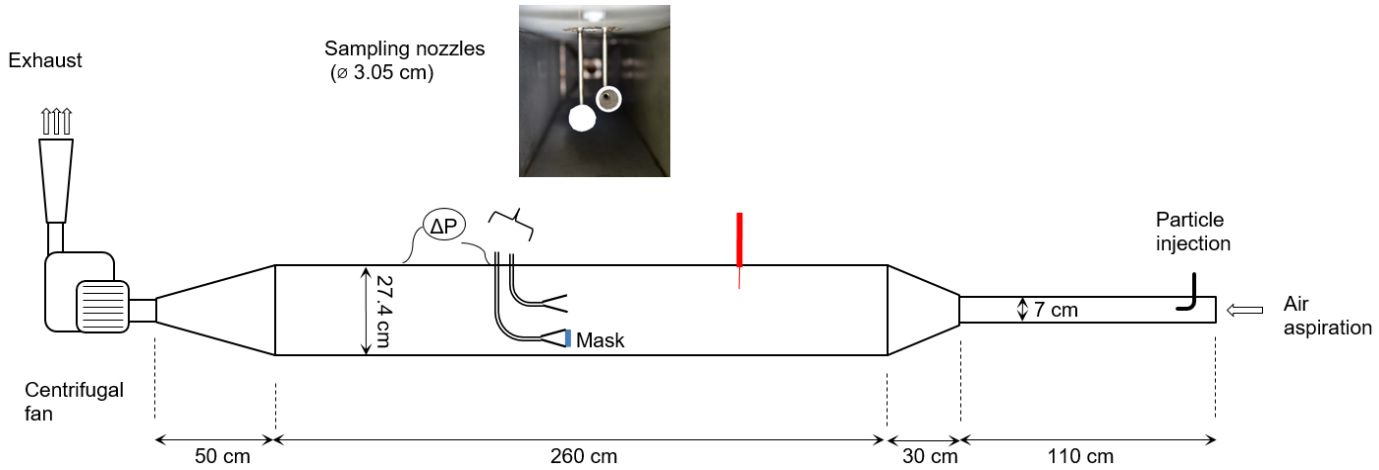

Fig. 1. Schematic of mask filtration efficiency measurement setup.

duct 260 cm long with a 27.4 cm × 27.4 cm cross-section, in which the velocity was kept constant at 9.6 cm s^{-1}. Two particle sampling probes were positioned 250 cm from the aerosol injection probe in the center of the square duct section. For the filtration test, the face mask material was fixed at the inlet section of one of the probes (Fig. 1) and a particle counter was connected to each of the two sampling probes in turn, for sampling upstream (empty probe) and downstream (probe with mask sample) of the mask filtering material respectively. The particle counting method is equivalent to the filter/dummy technique. Considering the mask material area set at 7.3 cm^2 (nozzle diameter set at 3.05 cm due to technical constraints of size and insertion in the experimental device) and the flowrate provided by the particle counter of 5 L min^{-1}, the filtration velocity was 11.4 cm s^{-1} (close to the filtration velocity of 9.6 cm s^{-1} recommended by EN 14683:2019). The mask pressure drop was measured using a differential pressure drop sensor connected to the probe containing the mask material.

2.2 Mask Tested

The medical face mask used for this study was type IIR (EN 14683:2019) manufactured by CA Diffusion. The same masks were tested by Alcaraz *et al.* (2022) to investigate technical solutions (washing cycles followed or not by autoclaving cycles) for the reuse of medical face masks in domestic and community setting. The mask was composed of three layers of non-woven polypropylene fiber materials: spunbond, meltblown, spunbond. The meltblown layer was positively and negatively charged by corona effect before assembly. Samples of the filtering material were tested before and after discharge of the electrostatic charges by exposure to isopropanol vapor, in accordance with the protocol for standard air filters used in general ventilation (ISO 16890-4). It should be noted that no experimental measurement of the electrical charge carried by the masks was carried out during the study to validate the complete media neutralization procedure.

The structural properties of the mask filtering material were characterized: media thickness (*Z*) and fiber diameter were quantified by SEM observation and picture analysis using ImageJ.

The differential pressure generated by flow through the filtering material was estimated by measuring the pressure drops for four increasing filtration velocities in the range from 9.4 to 11.4 cm s^{-1}, corresponding to the Welas (Palas) particle counter sample rate of between 4.1 and 5 L min^{-1}. For comparison purposes, a linear extrapolation of the results was carried out using a Darcy flow regime, in accordance with the Pore Reynolds number range, for a filtration velocity of 27 cm s^{-1} and a sample surface area of 4.9 cm^2, as stated in the EN 14683:2019 standard. Permeability (B) was estimated from the experimental media pressure drop value relating to a filtration velocity value of 11.4 cm s^{-1}, in accordance with Darcy's law (Eq. (1)).

$$B = \mu.Z.\frac{V_f}{\Delta P} \quad (1)$$

with μ the air viscosity (Pa s), ΔP the pressure drop (Pa), Z the thickness (m) and V_f the filtration velocity (m s^{-1}).

2.3 Test Aerosols: Nature, Generation and Counting

Five test aerosols were selected to cover the completeness of the current standards, the laboratory practicies and the physical properties in particular in terms of density, morphology, solid/liquid and inert/microbial particles:

- Di-ethyl-hexyl-sebacat (DEHS): liquid aerosol with a long lifetime (no evaporation) and spherical in shape.
- Alumina particles (Al_2O_3): solid aerosol composed of particles of irregular shape (Buehler 5-micron Ref: 40-6606-060-080).
- HOLI powder corn starch: solid aerosol composed of non-toxic corn starch particles of irregular shape (HoliFrance Ref: 2KGHFLUOJ).
- Sodium chloride (NaCl): solid aerosol of regular cubic shape.
- *Staphylococcus epidermidis* (CIP 81.55): aerosol from a non-pathogenic bacterial suspension of 0.5×10^7 CFU mL^{-1} diluted with peptone water.

In addition, to evaluate the efficiency of medical face masks against respiratory viruses, an aerosol of the non-enveloped bacteriophage *Emesvirus zinderi* (MS2) was used as a surrogate of pathogenic viruses (Whiley *et al.*, 2020).

The DEHS aerosol was produced by two generators simultaneously: a MAG 3000 (Palas) which generates condensation from DEHS vapour at 300°C, and an AGK 2000 (Palas) which atomizes the liquid DEHS. The alumina particles were generated by a rotating brush powder disperser RBG 1000 (Palas). The HOLI particles were generated by two alternate generators: i) powder dispersion with an RBG 1000 (Palas), ii) atomization of the suspension (25 g L^{-1} in water) with the AGK 2000. The NaCl particles were generated by atomizing a solution of 10 g L^{-1} in water with the AGK 2000. The bacterial suspension of *Staphylococcus epidermidis* was generated with the AGK 2000 in peptone water.

The particle number size distribution (PNSD) of the aerosols and spectral filtration efficiency of the masks (i.e., filtration efficiency discretized by particle diameters) were quantified by particle counters. Three different particle counters were compared: the Electrical Low-Pressure Impactor (ELPI, Dekati), the Aerodynamic Particle Sizer (APS 3321, TSI) and the Welas (Welas digital 2100, Palas). These three spectrometers with high time resolutions are widely used. The size classification in the ELPI and APS is related to the aerodynamic equivalent diameter, which is the relevant diameter for particle transport, and particle deposition for sizes larger than about 0.5 μm (Pagels *et al.*, 2005). The Welas, based on optical diameters, operates with a white light source and a 90° scattering angle detector to measure the light redirected by the particles.

The refractive index and density of the aerosols tested are given in Table 1.

The aerosols were generated on the test bench without prior neutralization. The aerosol charges were quantified by measuring the currents detected at the surface of the ELPI stages, by switching the charger on and off. The average charge q_k of the particles collected at stage k was calculated using Eq. (2).

$$q_k = \frac{I_k}{N_k \times q} \tag{2}$$

where I_k is the current (A) detected at stage k of ELPI with the inlet charger switched off, N_k the particle number concentration (part. m^{-3}) detected at stage k with the inlet charger switched on, and q the ELPI flow-rate volume (10 L min^{-1}). The results are expressed by the ratio q_k/e where e is the elementary charge (1.602×10^{-19} C). Note that for each ELPI stage, the charge measurement is an average value. It is therefore not possible to determine the distribution of neutral, positive and negative particles in a given stage.

The total number concentration for a given mean diameter $\overline{dp_i}$ corresponds to the sum of particle numbers measured for 3 successive channels. The channels considered (shown in Table S1) are those for which particles were detected for at least one test aerosol, i.e., from 0.221 to 3.398 μm

Table 1. Refractive index and density of aerosols tested.

	DEHS	Alumina	NaCl	*S. epidermidis* (peptone water)	HOLI
Density (g cm^{-3})	0.912	3.95	2.16	1.8*	1.5**
Refractive index (-)	1.45	1.78	1.54	n.s.	1.58

* www.carlroth.com/com/en/special-media/peptone-water-buffered/p/ace67.2
** www.fishersci.com/shop/products/corn-starch-2/S25580

for Welas and from 0.542 to 7.234 μm for APS. In terms of optical measurements with the Welas, total number concentrations were discarded for values < 30 part. cm^{-3}. With the APS, no values were discarded as the minimum particle concentration detectable is 0.001 part. cm^{-3}.

2.4 Particle Filtration Methodology

The Table 2 summarizes the various tests carried out. Each condition was tested 3 times (N = 3 samples of mask material) with several particle counts upstream (up) and downstream (down) of the mask material, up1/down1/up2/down2/up3/down3/up4, allowing calculation of j = 3 efficiency values. The sampling duration was 30 s for both particle counters, and the interval between each measurement was 15 s. Note that the particle counters used (Welas and APS) have a sampling flow rate of 5 L min^{-1}.

The average filtration efficiency value $E_{\overline{dp_i}}$ for particles with a mean diameter $\overline{dp_i}$ was calculated as N × j = 9 values using Eq. (3).

$$E_{\overline{dp_i}} = \frac{1}{9}\sum_{N=1}^{3}\sum_{j=1}^{3} E_{\overline{dp_i}} = \frac{1}{9}\sum_{N=1}^{3}\sum_{j=1}^{3}\left(\frac{\overline{C}_{up,j,\overline{dp_i}} - C_{down,j,\overline{dp_i}}}{\overline{C}_{up,j,\overline{dp_i}}}\right) \quad (3)$$

where N is the mask sample number, j the efficiency measurement number carried out by mask sample, $C_{down,j,\overline{dp_i}}$ the concentration number for particles with a mean diameter $\overline{dp_i}$ downstream of the mask material, i.e., with sampling probe 2, for measurement j, $\overline{C}_{up,j,\overline{dp_i}}$ is the average concentration number for particles with a diameter of $\overline{dp_i}$ upstream of the mask material, i.e., with sampling probe 1, calculated from the two measurements before and after downstream measurement j (Eq. (4)).

$$\overline{C}_{up,j,\overline{dp_i}} = \frac{C_{up,j,\overline{dp_i}} + C_{up,j+1,\overline{dp_i}}}{2} \quad (4)$$

Table 2. Synthesis of particle filtration efficiency tests.

	DEHS	Alumina	HOLI		NaCl	*S. epidermidis*	
	Condensation + atomization (MAG 3000 Palas + AGK 2000 Palas)	Powder dispersion (RBG1000 Palas)	Powder dispersion (RBG1000 Palas)	Suspension atomization (AGK 2000 Palas)	Solution atomization (AGK 2000 Palas)	Suspension atomization (AGK 2000 Palas)	Counter/ equivalent diameter
Unused charged face mask material	x	x	x	x	x	n.d.	Welas Palas/ optical diameter
	x	x	x	n.d.	x	x	APS TSI/ aerodynamic diameter
Unused discharged face mask material	x	x	x	x	x	n.d.	Welas Palas/ optical diameter

For measuring filtration efficiency, the pressure drop generated by mask samples subjected to the airflow was measured to ensure the masks did not clog.

For the tests carried out with the powder disperser RBG1000 (alumina and HOLI), the average efficiency was only calculated from the first efficiency value $j = 1$ measured for N samples of mask material, due to a small increase in pressure drop in the filtering media observed during the tests (maximum increase of 10% with HOLI powder for $j = 3$).

In order to guarantee a reliable comparison of results, precautions were taken in terms of device calibration, cleaning of the set-up, applying a rigourous protocol, checking the mask integrity, and proper fixation on the sampling nozzle.

2.5 Microbial Filtration Methodology

The MS2 bacteriophage was suspended in a buffer solution composed of NaCl, $MgSO_4$ and Tris-HCl, with the pH adjusted to a neutral value of 7. The solution was then atomized and dispersed in the test bench using the AGK 2000 (Palas) generator equiped with drier, maintaining the same airflow conditions as the particle filtration efficiency test. In contrast, the size of the sampling nozzles was 43 cm^2 to meet the isokinetic condition of the microbial sampling pump flow rate of 28.3 L min^{-1} by cascade impactors. Two identical six-stage viable cascade impactors (Tish) were connected synchronously to the upstream (empty) and downstream (covered with a mask sample) with respective sampling time of 3 and 6 min. For a given mask sample, $j = 3$ successive measurements with cascade impactors were performed. The impactors were implemented with petri dishes with a double agar layer, containing solid and soft agar culture medium suitable for *Escherichia coli* bacteria growth and lysis development when infected with MS2 bacteriophage. The microbial efficiencies of both charged and discharged mask materials were calculated by counting the lysis development after impaction and incubation for 24 h at 37°C.

The microbial filtration efficiency can be discretized by particle diameter considering the 6 stages of the cascade impactor (Whyte *et al.*, 2022b). The viral filtration efficiency $E_{PFU,k}$ for particles of MS2 impacted in the stage k of the six-stage viable particle sampler was calculated using Eq. (5) for charged or discharged masks.

$$E_{PFU,k} = \frac{1}{3}\sum_{N}\left(1 - \frac{\sum_{j=1}^{3} C_{PFU,stage\ k,down}}{\sum_{j=1}^{3} C_{PFU,stage\ k,up}}\right) \tag{5}$$

where N is the number of mask sample tested, j the Andersen measurement number carried out by mask sample, $C_{PFU,stage\ k,up}$ and $C_{PFU,stage\ k,down}$ the viral concentration expressed in PFU m^{-3} (plaque forming unit) collected on the stage k of the Andersen impactor respectively upstream and downstream of the mask tested.

The average viral filtration efficiency value E_{PFU} for particles of MS2 was calculated using Eq. (6).

$$E_{PFU} = \frac{1}{3}\sum_{N}\left(1 - \frac{\sum_{k=1}^{6}\sum_{j=1}^{3} C_{PFU,stage\ k,down}}{\sum_{k=1}^{6}\sum_{j=1}^{3} C_{PFU,stage\ k,up}}\right) \tag{6}$$

Reliable results were obtained for N = 2 with charged mask and N = 1 with discharged mask.

3 RESULTS

3.1 Characterization of Porous Structural Properties of Medical Mask Material

The total mean thickness of the medium, i.e., multilayer spunbond (SP)/meltblown (MB)/spunbond (SP), was estimated at 670 ± 60 μm (N = 5) with about 108 ± 17 μm (N = 23) for the MB layer.

The layers were composed of polydispersed unimodal polypropylene fibers with a mean fiber diameter of 2.0 ± 0.6 µm (N = 151 fibers analyzed) for the MB layer and 17 ± 2 µm (N = 56 fibers analyzed) for the SP layers. SEM observations of meltblow and spunbond layers are presented in Fig. S1.

The permeability of the filtering medium was estimated at (1.7 ± 0.2) × 10^{-11} m^2 in terms of total mean thickness and for Eq. (1). The mean differential pressure for face mask media is 38 ± 5 Pa cm^{-2}, i.e., less than the < 60 Pa cm^{-2} for the type IIR standard reported in the EN 14683:2019 standard.

3.2 Comparison of Particle Number Size Distribution of Test Aerosols Measured from Aerodynamic and Optical Particle Counters

Particle number size distributions (PNSD) for the various aerosols tested, expressed as aerodynamic diameter (APS and ELPI measurements) and optical diameter (Welas measurement), are shown in Fig. 2. Number median diameters d50 are reported in the figure. Note that for APS, the aerodynamic d_{50} was calculated using particles less than 0.5 µm detected by the particle counter but not discretized by size.

Particle size distribution differed depending on the counting method used and equivalent diameter involved. A shift was observed in the optical diameter curves in relation to the aerodynamic

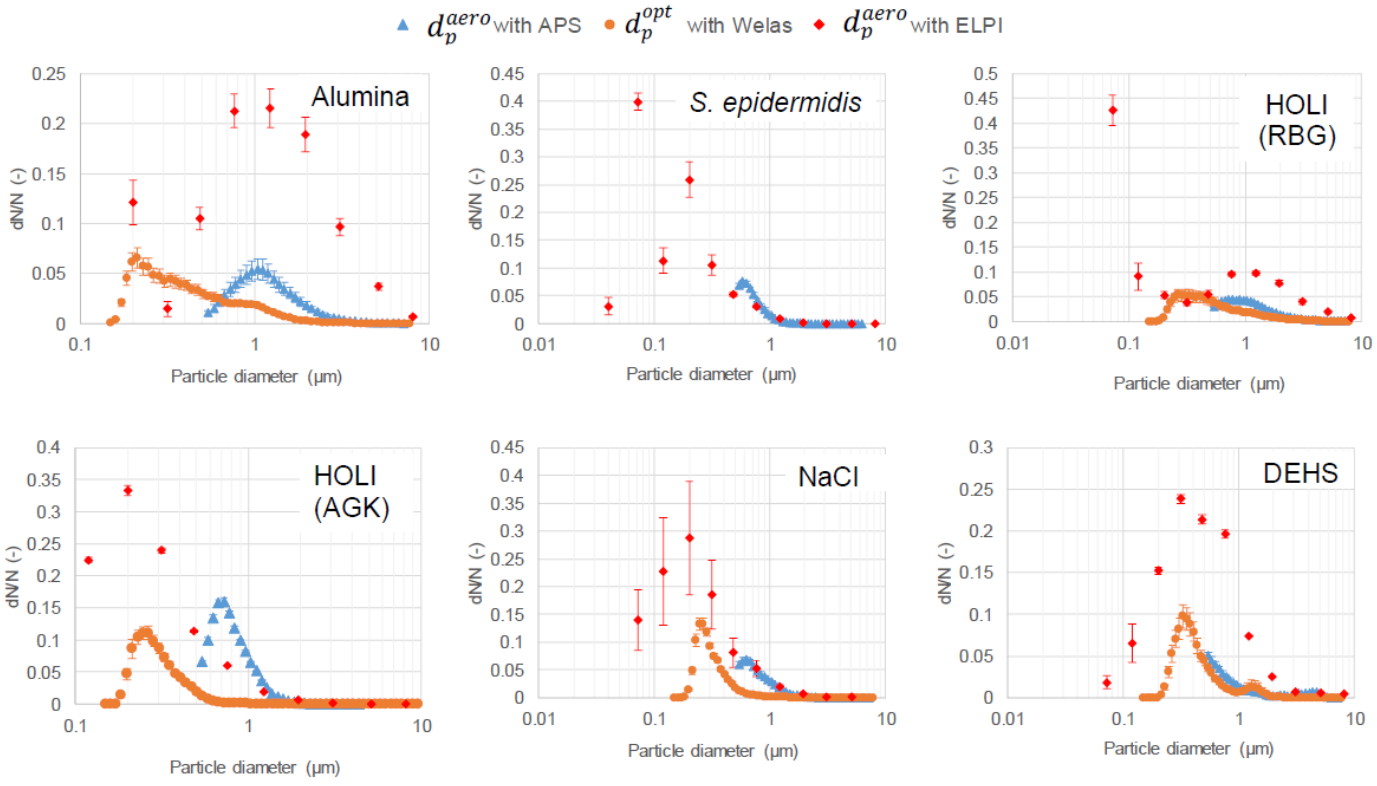

	HOLI RBG	HOLI AGK	DEHS AGK + MAG	NaCl AGK	Alumina RBG	*S. epidermidis* AGK
d_{50}^{opt} Welas (µm)	0.41	0.27	0.36	0.27	0.33	n.s.
d_{50}^{aero} APS (µm)	0.75	0.63	< 0.5	0.55	0.89	< 0.5

Fig. 2. Particle number size distributions and corresponding number median diameter d_{50} of test aerosols by APS and ELPI, expressed in aerodynamic diameters, and by Welas, expressed in optical diameters (average values ± standard deviation from N = 3 × 4).

diameter curves for all aerosols. The aerodynamic modal or median diameter was always greater than the optical diameter: e.g., the median diameter for HOLI powder generated by dry dispersion was 0.4 μm as opposed to 0.75 μm. The particle distribution shift was typically due to the density and non-sphericity of the particles (Eq. (7)); other parameters may also have an influence: the index of refraction used for the optical measurement and diffusivity of the particles, and the calibration of the devices and compatibility of the particle counter with liquid aerosols, for example.

$$\chi = \frac{\rho_p \times \left(d_p^{ev}\right)^2 \times Cu\left(d_p^{ev}\right)}{\rho_0 \times \left(d_p^{aero}\right)^2 \times Cu\left(d_p^{aero}\right)} \tag{7}$$

where χ is the dynamic shape factor of the particle, ρ_p the particle density, ρ_0 = 1000 kg m^{-3}, and $Cu\left(d_p^{ev}\right)$ and $Cu\left(d_p^{aero}\right)$ the Cunningham coefficients of the particle, expressed in equivalent volume and in aerodynamic diameter, respectively.

The results obtained for the two methods of generating HOLI powder indicate that the method of generation, i.e., dry, by powder dispersion or wet, by atomization of a suspension, influences the particle size distribution, with larger particles and more disperse distribution with dry generation than with atomization.

The results of the two aerodynamic diameter counters (APS and ELPI) demonstrate good concurrence of the PNSD measured with similar modal values. The two powders generated in dry mode, alumina and HOLI (using the RBG 1000 Palas), seem to display a second sub-micron mode outside the counting range of the APS counter. The three aerosols, NaCl, *S. epidermidis* and HOLI, generated by atomization, exhibit a gap between the two aerodynamic particle size distributions, with a lower modal diameter value when measured with the ELPI than with the APS.

The discrepancy between the two aerodynamic PNSDs from the APS and ELPI counters is observed for diameters smaller than 5 μm and having a density close to 2 g cm^{-3} (1.5–2.1 depending on the aerosol—see Table 1). This discrepancy is not observed for liquid spherical DEHS aerosols (density close to 1 g cm^{-3}) or solid alumina aerosols (density close to 4 g cm^{-3}) of irregular shape.

3.3 Comparison of Electrostatic Charges of Test Aerosols as a Function of Particle Diameter – Influence of Aerosol Nature and Generation Method

The average charges of the particles collected at stage *k* of the ELPI and normalized by the elementary charge q_k/e are shown in Fig. 3 for the various aerosols tested. The results demonstrate that charges vary depending on the nature of the aerosol and the particle diameter, with more charges measured for particle diameters above 1 μm. The DEHS aerosol remained close to neutrality whatever the particle diameter. HOLI and NaCl generated by atomization displayed mostly a low average negative charge, with the maximum average charge q_k close to 2 μm and low average positive charges close to 0.2 μm (HOLI) or 5 μm (NaCl) suggesting bipolar aerosols with positive/negative and maybe neutral particles. Alumina and *S. epidermidis* aerosols displayed negative charges that increased with particle diameter in the super-micron size range. The negative charges of alumina particles decreased from -1.8×10^{-18} to -7.6×10^{-18} C for aerodynamic diameters of between 2 and 5 μm (or Stokes diameters between 1 and 3 μm). HOLI generated by dry dispersion demonstrated low negative charges for particles in the sub-micron size range and significant positive charges for particles above around 1 μm, with an increase in particle charge from 1.1×10^{-18} to 4.9×10^{-18} C for aerodynamic of diameters of between 1.2 and 5 μm.

Note that the ELPI measures the average charge of the particles detected on each of the 12 stages. Particles with positive, negative or neutral charges cannot be discretized at the level of one stage. Thus, bipolar aerosols composed of particles with positive and negative charges cannot be reliably quantify for their charges with an ELPI with probably underestimation of their charges (e.g., HOLI and NaCl aerosols).

Moreover, the methodology to quantify the average particle charges on the ELPI stages supposes successive measurements with the charger switched on and off. The ELPI charger brings

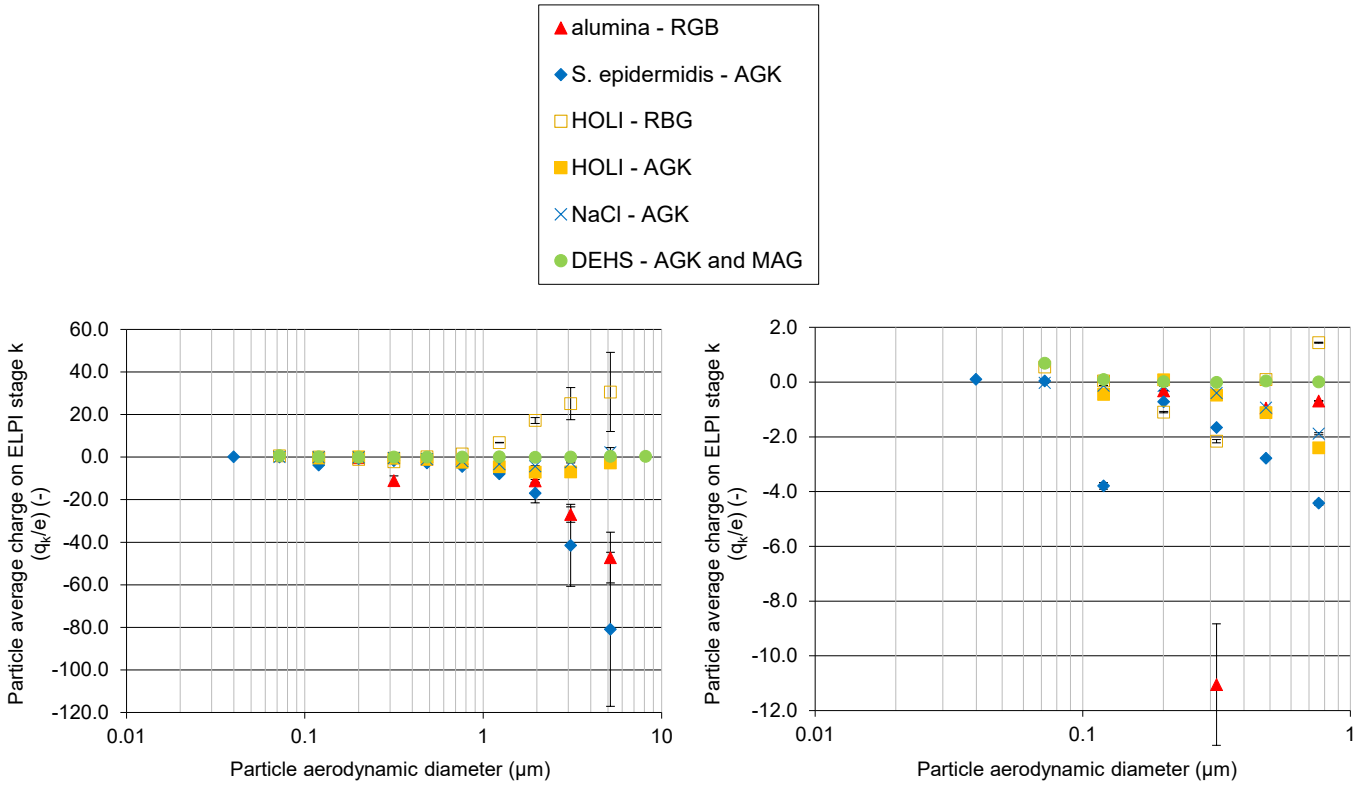

Fig. 3. Particle average charge (q_k/e) according to aerodynamic mean diameter of the ELPI stages - left: complete scale; right: focus on 0.01 to 1 µm particle diameter range (average value and standard deviation for 10 min sampling period).

positive charges to the aerosol tested and allows the characetrization of its PNSD possible. But for high negative particles, the PNSD may be underestimated because of not complete charging of the particles affecting also the quantification of q_k. For *S. epidermidis* for example, in particular for particle diameters > 1 µm, the charges seems to be fully negative but the q_k value (get with charger switched off) may be overestimated if the number of particles (get with charger switched on) was underestimated (Eq. (2)).

Despite the precautions to be considered, the results obtained with HOLI indicate that the method of generation, i.e., dry with powder dispersion or wet by atomization of a suspension, influences not only the particle size distribution but also the charges carried by the particles. The results also demonstrate opposing charges depending on the nature of the powder (alumina or HOLI) using the same powder dispersion generation system with a rotating brush (RBG 1000 Palas).

Forsyth *et al.* (1998) explained that the generation of aerosols by atomization promotes spray electrification. For KCl and NaCl aerosols, the authors observed that a higher molar salt concentration resulted in a lower charge level due to the effect of dissolved ions on the dipole charge layer at the liquid/gas interface. The results in Fig. 3 indicate that the charges for the bacterial suspension in peptone water were greater than those for the NaCl aerosol, probably because the salt concentration was lower in the bacterial suspension despite the presence of peptone.

Forsyth et al. (1998 observed that the dust particle contact potential and resulting electrical charge are dependent on the characteristics of the bulk material and the dispersion method. Contact charging occurs as a result of the disruption of a dust or powder surface during aerosol generation. A triboelectric or contact charge develops along the particle surface due to mechanical friction from the surface or particle contact during dispersion.

Rodrigues *et al.* (2006) observed opposing charges for alumina and diatomite particles generated with the same powder disperser with triboelectrical effect. The linear dependence of particle charges with particle diameters in the super-micron size range, as well as the order of magnitude of particle charges measured by Rodrigues *et al.* (2006), concurs with the results obtained with alumina and HOLI generated by powder dispersion.

3.4 Filtration Efficiency of Unused Charged Face Mask Material against Test Aerosols – Comparison of Results Based on Aerodynamic and Optical Diameters

The resulting filtration efficiencies of unused mask material containing electret media MB are given in Fig. 4 for the various aerosols tested.

The results show increasing filtration efficiency with increasing particle diameter between 0.25 and 1 µm for d_p^{opt} or between 0.6 and 2 µm for d_p^{aero}. In this part of the curve, the nature of the aerosol influences the filtration efficiency of the filtering material. In the super-micron particle size range, the impaction and interception mechanisms were predominant and filtration efficiency was close to 100% for all aerosols. The results expressed in aerodynamic diameter demonstrate the influence of particle nature (density and charge) on filtration efficiency:

– Alumina and HOLI generated by dry powder dispersion demonstrated a higher filtration efficiency for $d_p^{aero} < 1$ µm, followed by *S. epidermidis*. Despite the low density for HOLI and *S. epidermidis* aerosols, which limits collection by impaction in the diameter range concerned, the high filtration efficiency is explained by the charges of the aerosols enhancing collection by coulombic forces.
– DEHS and NaCl demonstrated lower filtration efficiency in the sub-micron particle size range, which may be explained by their low density and charge. Nevertheless, filtration efficiency was > 90% due to electrostatic enhancement by polarization forces.

Kulmala *et al.* (2021) observed the influence of particle charge on the filtration efficiency of medical face masks in the sub-micron size range. They investigated enhancement of the filtration efficiency of medical face mask media by charging the DEHS particles. They observed that the positive charging of particles with a unipolar corona charger significantly increased filtration efficiency in the sub-micron size range; however, they point out the need to optimize the process prior to practical application, by limiting ozone production via ionization, in order to avoid health risks.

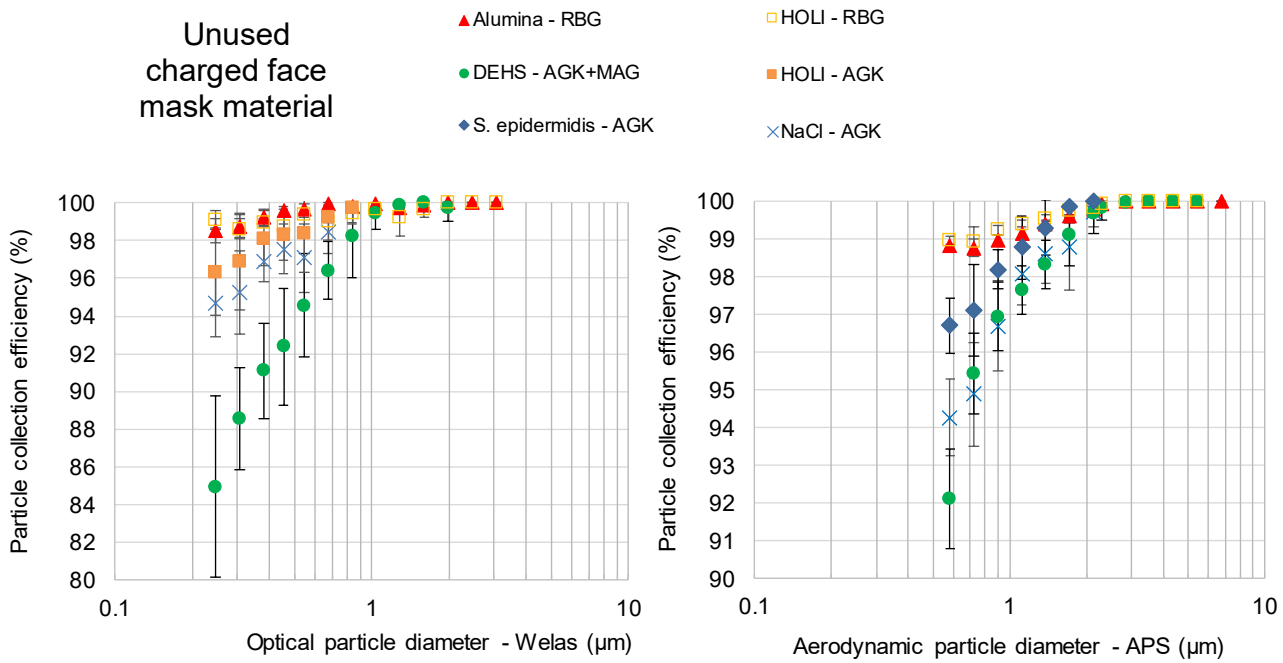

Fig. 4. Filtration efficiency of unused charged medical face mask material depending on particle diameter - left: optical diameter by Welas count; right: aerodynamic diameter by APS count (average value ± standard deviation N = 3 samples).

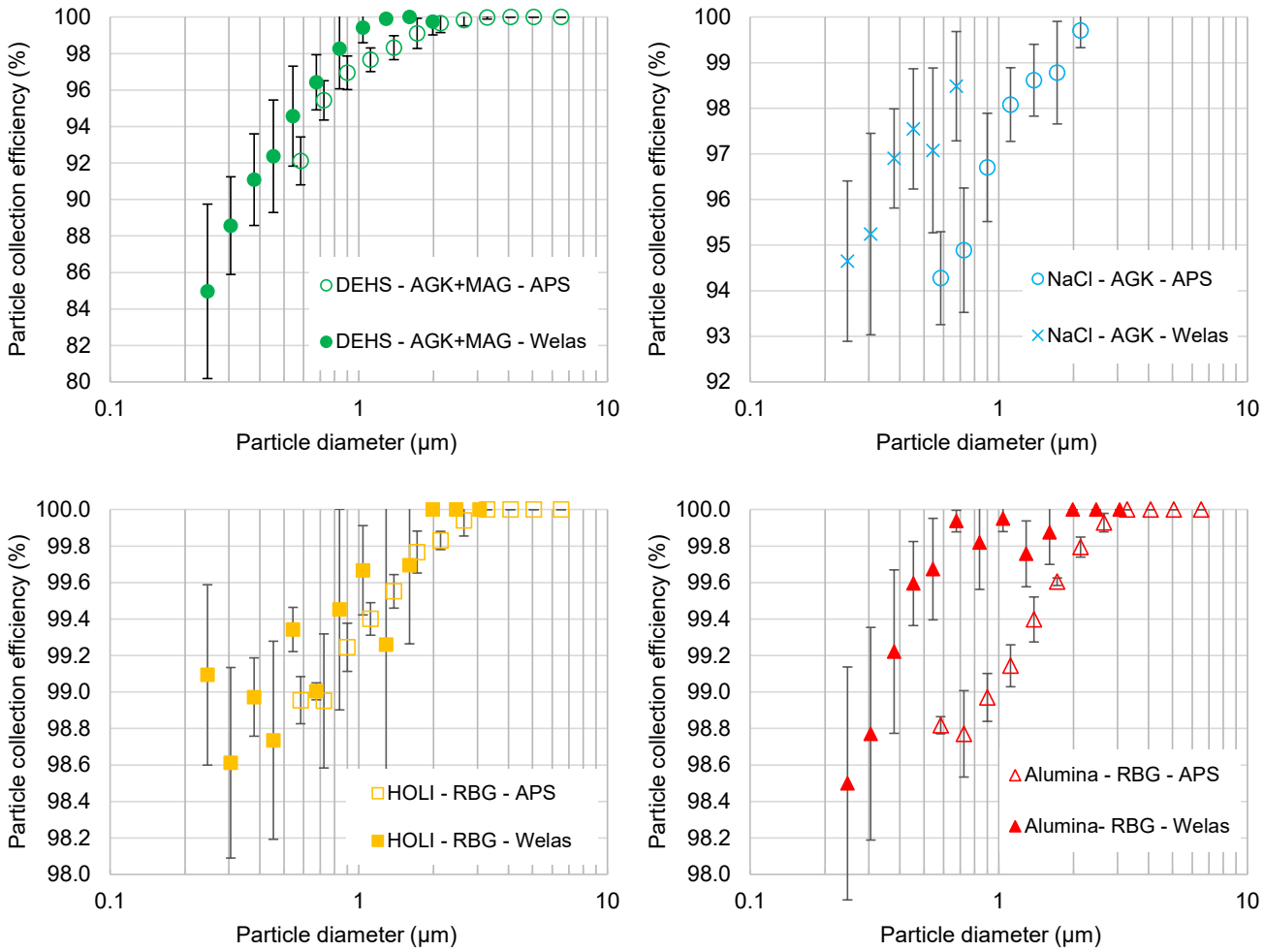

Fig. 5. Comparison of filtration efficiency of unused charged medical face mask material against particle diameters, using APS and Welas measurements (average value ± standard deviation N = 3 samples).

The filtration efficiencies obtained using the Welas optical particle counter were compared to the ones obtained by the APS aerodynamic counter for the several aerosols tested in Fig. 5 (except *S. epidermidis* and HOLI generated by atomization, due to missing experimental data). The results demonstrate a shift in the spectral filtration efficiency between the data express in optical or aerodynamic diameter. The shift is mainly attributed to the dynamic shape factor and density of the particles (Eq. (7)). For DEHS aerosol, the shift is negligible because of dynamic shape factor (sphere) and density close to 1. In contrast, the mineral alumina particles whose shapes are irregular, display a significant shift between efficiency expressed in optical or aerodynamic diameters as previsouly observed for the PNSD in Fig. 2.

The MPPS of the mask material could be identified by completing the efficiency measurements with a particle electrical mobility counter (Whyte *et al.*, 2022a).

3.5 Filtration Efficiency of Unused Discharged Face Mask Material against Test Aerosols from Optical Diameters – Comparison of Unused Charged and Discharged Face Mask Material

The filtration efficiencies of discharged mask material were compared to those of charged filtering material in Fig. 6 (except *S. epidermidis*). The results reveal a significant drop in filtration efficiency for sub-micron particles where none of the particle collection mechanisms are dominant.

The filtration efficiencies of discharged mask material for the several aerosols tested obtained

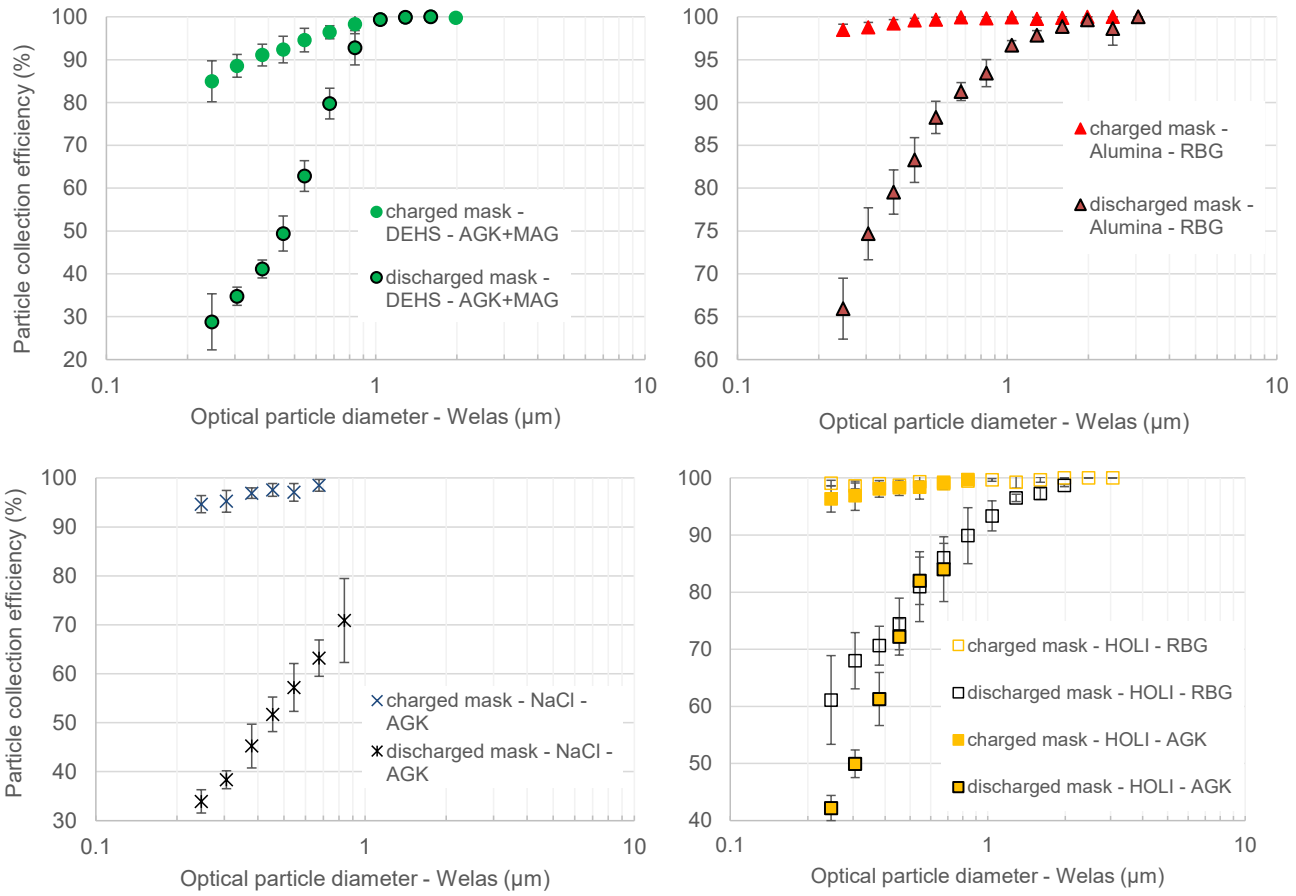

Fig. 6. Comparison of filtration efficiencies of charged and discharged medical face mask material using optical particle diameters from Welas measurements (average value ± standard deviation N = 3 samples).

with the optical particle counter are presented in Fig. 7. The results confirm the influence of the aerosol nature, in particular aerosol charges on particle co llection efficiency in the sub-micron size range. For particles in the size range 0.3 to 0.8 µm, two categories of aerosol can be distinguished:

– The discharged mask material showed a collection efficiency > 60% for alumina and HOLI particles generated by dry dispersion; despite the fibers being discharged, particles were still collected by electrostatic force via image force due to their charge.
– The filtration efficiencies of DEHS, HOLI AGK and NaCl are lower (minimum value 30%), collection by electrostatic effect being almost non-existent.

3.6 Comparison of Viral Filtration Efficiency to NaCl Particle Efficiency for Charged and Discharged Medical Face Mask Material according to Aerodynamic Particle Diameter

The virus was detected upstream of the mask on the 6 stages of the cascade impactor with an average virus diameter of 2.1 ± 0.06 µm. The particle size distribution is presented in Fig. S2. This result suggests that the bacteriophage is unlikely to be transported alone, but rather, the aggregation or adsorption of the MS2 virus on NaCl particles forming the solution particles is more probable.

The total average viral filtration effiency was 98.5 ± 0.4% versus 81.8% respectively for the charged and the discharged mask materials. Fig. 8 presents the spectral MS2 microbial filtration efficiency for charged and discharged mask materials discretized by the 6 impactor stages. The results were compared with the spectral particle collection efficiency of NaCl expressed in aerodynamic diameter. For discharged mask, the expremental data for NaCl filtration efficiency

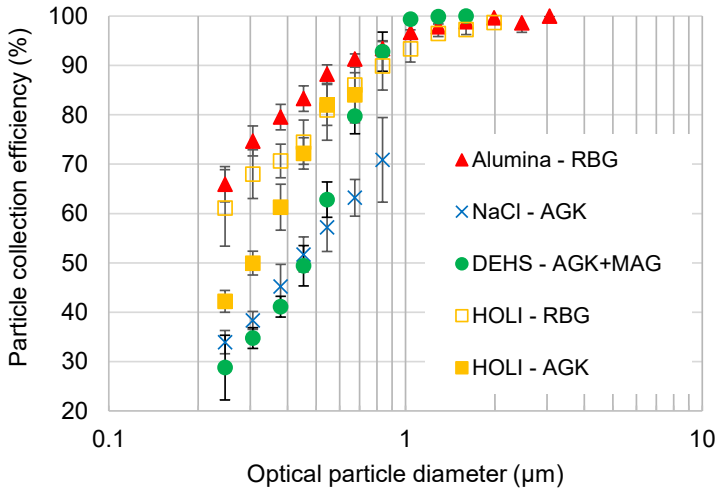

Fig. 7. Filtration efficiency of unused discharged medical face mask material depending on optical particle diameter (average value ± standard deviation N = 3 samples).

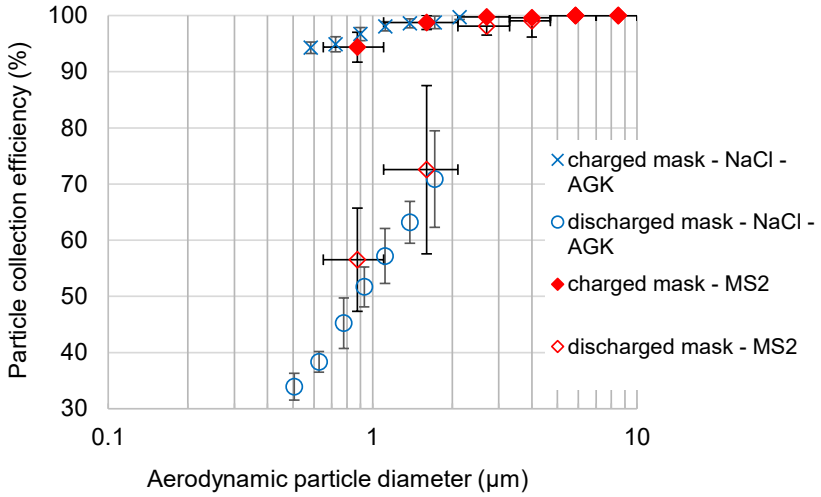

Fig. 8. Comparison of viral filtration efficiency to NaCl particle efficiency for charged and discharged medical face mask material according to aerodynamic particle diameter.

was determined from optical counting. The filtration efficiencies obtained using the Welas counter were expressed as aerodynamic diameters by comparing PNSDs. A shift coefficient was applied to the different Welas diameter channels in order to correlate the median diameters of the two PNSDs i.e., the original aerodynamic distribution by APS and the aerodynamic distribution calculated by Welas. This procedure assumes that for a given aerosol, the density and dynamic shape factors are the same whatever the particle diameter. The results demonstrated a clear concordance between MS2 and NaCl particle filtration efficiency for a same aerodynamic diameter for charged and discharged mask material. This concordance may be attributed to the use of comparable saline solutions.

3.7 Discussion - Importance of Electrostatic Forces in Aerosol Filtration with Medical Face Mask, and What Affects them in Test Protocols

The results demonstrate the influence of electrostatic forces on the filtration efficiency of materials used in medical face masks tested for aerosol charge level and initial charge of the filtering medium.

The initial charge of the filtering medium has a significant influence on filtration efficiency for particles in the sub-micron size range: filtration efficiency drops by a few percentage points in the case of neutral particles in particular, when the filtering material is discharged (Fig. 6).

For aerosols in the sub-micron size range, the charge affects collection by filtering material which is charged (Fig. 4), and also when it has been discharged (Fig. 7). The issue of how representative test aerosols can be of droplets actually emitted by mask wearers, in terms of electrostatic forces, is of particular relevance. Saliva is typically composed of electrolytes (including sodium, potassium, calcium, magnesium, bicarbonate and phosphates), immunoglobulins, proteins, enzymes, mucins and nitrogenous products (urea and ammonia) (Humphrey and Williamson, 2001).

The charge of saliva therefore suggests that filtering droplets containing viruses through an electret filtering material such as a medical face mask cannot be mimic by a neutral aerosol which would underestimate the filtration efficiency, for sub-micron particles in particular, as suggested in Fig. 4.

The occurrence of viral particles in the sub-micron size range demands characterization of the collection efficiency of medical face masks within this range, or at least the efficiency of the filtering material, i.e., for particles less than 3 μm, optimally in the MPPS zone of the filtering media.

The current European standard focuses on the bacterial filtration efficiency of filtering materials for *S. aureus* in the 3.0 μm diameter range, whereas the US standard also considers particle filtration efficiency at 0.1 μm with neutralized latex particles. The issue of how representative test aerosols are of droplets emitted by mask wearers is a particular issue in the standards. Considering the significant influence that the absolute charge of the test aerosols has on filtration performance in the sub-micron size range, the test protocol must be well-defined in terms of the nature of the aerosols and the means of generating them in order to clarify their absolute charge level. The use of neutralized aerosols enables quantification of the filtration performance in unfavorable conditions for particles in the sub-micron size range, i.e., by reducing collection by electrostatic forces. This is the test protocol established by the ISO 16890:2017 standard for HVAC filters which considers the spectrum of particle size efficiency in the range 0.3 to 10 μm using neutralized filtering media, and requires two test aerosols: DEHS and KCl neutralized after generation (ISO 16890-2). The reason for using neutralized media and neutral aerosols in the test protocol is explained by the use of electret filters, which are becoming more common in air handling units. Filters lose their charge over their lifetime, which can be up to one year of use, when they are exposed to a humid air flow or temperature. The standard therefore evaluates the efficiency of the filter under the most unfavorable conditions. In terms of medical face masks, the standards could integrate a minimum filtration efficiency after testing with neutral particles and neutralized filtering material.

4 CONCLUSIONS

The physical properties of aerosols are greatly influenced by the method used to generate them, affecting consequently the efficiency with which they can be collected by filtering media such as medical face masks. The results have shown that the particle size distribution and particle charges for a given type of aerosol can differ depending on the generator used, in particular the wet or dry nature of generation. The aerodynamic diameter enables comparison of the filtration efficiencies of aerosols of various natures. The filtration efficiency of medical face mask material, composed of polypropylene layers and assimilated with an electret filter, is positively influenced by the charges of the aerosol. The filtration efficiency of neutral aerosols (e.g., DEHS) by unused charged face mask material is lower in the sub-micron particle range than that of charged aerosols (e.g., alumina) due to the electrostatic forces (polarization forces versus coulombic forces) which enhance filtration efficiency: 92% versus 99% efficiency for DEHS and alumina respectively, for a mean aerodynamic diameter of 0.6 μm. With discharged face mask material, the difference is higher: 30% versus 65% efficiency for a mean optical diameter of 0.25 μm and respectively for DEHS and alumina, for which image force can enhance collection. For particle sizes > 3 μm, the results indicate that the nature of the test aerosol has little influence because particle collection is dominated by the impaction and interception mechanisms. Regarding the tests with MS2 virus,

the results demonstrated a good fit between MS2 and NaCl particle filtration efficiencies expressed in aerodynamic diameters and ranged between 0.65 and > 7 μm, for charged and discharged medical face mask material.

SUPPLEMENTARY MATERIAL

Supplementary material for this article can be found in the online version at https://doi.org/10.4209/aaqr.230180

REFERENCES

Alcaraz, J.P., Le Coq, L., Pourchez, J., Thomas, D., Chazelet, S., Boudry, I., Barbado, M., Silvent, S., Dessale, C., Antoine, F., Guimier-Pingault, C., Cortella, L., Rouif, S., Bardin-Monnier, N., Charvet, A., Dufaud, O., Leclerc, L., Montigaud, Y., Laurent, C., Verhoeven, P., *et al.* (2022). Reuse of medical face masks in domestic and community settings without sacrificing safety: Ecological and economical lessons from the Covid-19 pandemic. Chemosphere 288, 132364. https://doi.org/10.1016/j.chemosphere.2021.132364

Bahloul, A., Brochot, C., Layne, B. (2021). Leakage versus material filtration in barrier facemask Efficiency. Health 13, 439–453. https://doi.org/10.4236/health.2021.134035

Baker, R.E., Mahmud, A.S., Miller, I.F., Rajeev, M., Rasambainarivo, F., Rice, B.L., Takahashi, S., Tatem, A.J., Wagner, C.E., Wang, L.F., Wesolowski, A., Metcalf, C.J.E. (2022) Infectious disease in an era of global change. Nat. Rev. Microbiol. 20, 193–205. https://doi.org/10.1038/s41579-021-00639-z

Brown, R.C. (1993). Air filtration: An integrated approach to the theory and applications of fibrous filters (1st ed). Pergamon Press.

Dahneke, B. (1971). The capture of aerosol particles by surfaces. J. Colloid Interface Sci. 37, 342–353. https://doi.org/10.1016/0021-9797(71)90302-X

Davies, C.N. (1973). Air filtration. Academic Press.

EN 14683+A1:2019 (2019). Medical face masks—Requirements and test methods.

EN 149:2009 (2009). Respiratory protective devices—Filtering half masks to protect against particles—Requirements, testing, marking.

EN ISO 16890-2:2016 (2016). Air filters for general ventilation—Part 2: Measurement of fractional efficiency and air flow resistance.

EN ISO 16890-4:2016 (2016). Air filters for general ventilation—Part 4: Conditioning method to determine the minimum fractional test efficiency.

Forsyth, B., Liu, B.Y.H., Romay, F.J. (1998). Particle charge distribution measurement for commonly generated laboratory aerosols. Aerosol Sci. Technol. 28, 489–501. https://doi.org/10.1080/02786829808965540

Humphrey, S.P., Williamson, R.T. (2001). A review of saliva: Normal composition, flow, and function. J. Prosthet. Dent. 85, 162–169. https://doi.org/10.1067/mpr.2001.113778

Kähler, C.J., Hain, R. (2020). Fundamental protective mechanisms of face masks against droplet infections. J. Aerosol Sci. 148, 105617. https://doi.org/10.1016/j.jaerosci.2020.105617

Kulmala, I., Heinonen, K., Salo, S. (2021). Improving filtration efficacy of medical face masks. Aerosol Air Qual. Res. 21, 210043. https://doi.org/10.4209/aaqr.210043

Liu, Y., Ning, Z., Chen, Y., Guo, M., Liu, Y., Gali, N.K., Sun, L., Duan, Y., Cai, J., Westerdahl, D., Liu, X., Xu, K., Ho, K., Kan, H., Fu, Q., Lan, K. (2020). Aerodynamic analysis of SARS-CoV-2 in two Wuhan hospitals. Nature 582, 557–560. https://doi.org/10.1038/s41586-020-2271-3

Pagels, J., Gudmundsson, A., Gustavsson, E., Asking, L., Bohgard, M. (2005). Evaluation of aerodynamic particle sizer and electrical low-pressure impactor for unimodal and bimodal mass-weighted size distributions. Aerosol Sci. Technol. 39, 871–887. https://doi.org/10.1080/02786820500295677

Prather, K.A., Wang, C.C., Schooley, R.T. (2020). Reducing transmission of SARS-CoV-2. Science 368, 1422–1424. https://doi.org/10.1126/science.abc6197

Rodrigues, M.V., Marra Jr., W.D., Almeida, R.G., Coury, J.R. (2006). Measurement of the electrostatic

charge in airborne particles: II - particle charge distribution of different aerosols. Braz. J. Chem. Eng. 23, 125–133. https://doi.org/10.1590/S0104-66322006000100014

Romay, F.J., Liu, B.Y.H., Chae, S.J. (1998). Experimental study of electrostatic capture mechanisms in commercial electret filters. Aerosol Sci. Technol. 28, 224–234. https://doi.org/10.1080/02786829808965523

Spielman, L.A. (1977). Particle capture from low-speed laminar flows. Annu. Rev. Fluid Mech. 9, 297–319. https://doi.org/10.1146/annurev.fl.09.010177.001501

Wang, C.S. (2001). Electrostatic forces in fibrous filters—A review. Powder Technol. 118, 166–170. https://doi.org/10.1016/S0032-5910(01)00307-2

Whiley, H., Keerthirathne, T.P., Nisar, M.A., White, M.A.F., Ross, K.E. (2020). Viral filtration efficiency of fabric masks compared with surgical and N95 masks. Pathogens 9, 762. https://doi.org/10.3390/pathogens9090762

Whyte, H.E., Joubert, A., Leclerc, L., Sarry, G., Verhoeven, P., Le Coq, L., Pourchez, J. (2022a). Reusability of face masks: Influence of washing and comparison of performance between medical face masks and community face masks. Environ. Technol. Innovation 28, 102710. https://doi.org/10.1016/j.eti.2022.102710

Whyte, H.E., Joubert, A., Leclerc, L., Sarry, G., Verhoeven, P., Le Coq, L., Pourchez, J. (2022b). Impact of washing parameters on bacterial filtration efficiency and breathability of community and medical facemasks. Sci. Rep. 12, 15853. https://doi.org/10.1038/s41598-022-20354-w

YY/T 0469 (2011). Surgical mask. Pharmaceutical industry standard of the people's republic of China. China Food and Drug Administration, China.